https://doi.org/10.5194/acp-2019-1198
Preprint. Discussion started: 9 March 2020

Atmospheric Chemistry and Physics Discussions

Spatial and temporal representativeness of point measurements for nitrogen dioxide pollution levels in cities

Ying Zhu[a,b], Jia Chen[b], Xiao Bi[b], Gerrit Kuhlmann[c], Ka Lok Chan[d], Florian Dietrich[b], Dominik Brunner[c], Sheng Ye[a], and Mark Wenig[a]

[a]Meteorological Institute, Ludwig-Maximilians-Universität München, Munich, Germany
[b]TUM Department of Electrical and Computer Engineering, Technische Universität München, Munich, Germany
[c]Empa, Swiss Federal Laboratories for Materials Science and Technology, Überlandstrasse 129, Dübendorf, Switzerland
[d]Remote Sensing Technology Institute (IMF), German Aerospace Center (DLR), Oberpfaffenhofen, Germany

Correspondence: Y.Zhu (ying.zhu@physik.uni-muenchen.de), M.Wenig (mark.wenig@lmu.de), J.Chen (jia.chen@tum.de)

Abstract. In many cities around the world the overall air quality is improving, but at the same time nitrogen dioxide (NO_2) trends show stagnating values and in many cases could not be reduced below air quality standards recommended by the World Health Organization (WHO). Many large cities have built monitoring stations to continuously measure different air pollutants. While most stations follow defined rules in terms of measurement height and distance to traffic emissions, the question remains, how representative are those point measurements for the city-wide air quality. The question of the spatial coverage of a point measurement is important because it defines the area of influence and coverage of monitoring networks, determines how to assimilate monitoring data into model simulations or compare to satellite data with a coarser resolution, and is essential to assess the impact of the acquired data on public health.

In order to answer this question, we combined different measurement data sets consisting of path averaging remote sensing data and in-situ point measurements in stationary and mobile setups from a measurement campaign that took place in Munich, Germany in June and July 2016. We developed an algorithm to strip temporal diversity and spatial patterns, in order to construct a consistent NO_2 pollution map for Munich. Continuous long-path differential optical absorption spectroscopy (LP DOAS) measurements were complemented with mobile cavity-enhanced (CE) DOAS, chemiluminescence (CL) and cavity attenuated phase shift (CAPS) instruments and were compared to monitoring stations and satellite data. In order to generate a consistent composite map, the LP DOAS diurnal cycle has been used to normalize for the time of the day dependency of the source patterns, so that spatial and temporal patterns can be analyzed separately. The resulting concentration map visualizes pollution hot spots at traffic junctions and tunnel exits in Munich, providing insights into the strong spatial variations. On the other hand, this database is beneficial to the urban planning and the design of control measures of environment pollution. Directly comparing on-street mobile measurements in the vicinity of monitoring stations resulted in a difference of $48\,\%$. For the extrapolation of the monitoring station data to street level, we determined the influence of the measuring height and distance to the street. We found that a measuring height of $4\,\mathrm{m}$, at which the Munich monitoring stations measure, results in $16\,\%$ lower average concentrations than a measuring height of $1.5\,\mathrm{m}$, which is the height of the inlet of our mobile measurements and a typical pedestrian breathing height. The horizontal distance of most stations to the center of the street of about $6\,\mathrm{m}$ also results in an average reduction of $13\,\%$ compared to street level concentration. A difference of $21\,\%$ in the NO_2 concentrations

https://doi.org/10.5194/acp-2019-1198
Preprint. Discussion started: 9 March 2020

Atmospheric Chemistry and Physics Discussions

remained, which could be an indication that city-wide measurements are needed for capturing the full range and variability of concentrations for assessing pollutant exposure and air quality in cities.

1 Introduction

Many former studies (Huang et al., 2014; Dunlea et al., 2007; Jang and Kamens, 2001) have been pointed out that NO_2 is an important composition in the process of both tropospheric and stratospheric chemistry. It is one of the major pollution products from combustion processes. Catalytic formation of tropospheric ozone (O_3) and the formation of secondary aerosols that cause acid rain, all of which involve its participation. Elevated concentration of atmospheric NO_2 is acknowledged to be noxious to human beings health. In urban environments, Exhaust emissions are one of the primary sources of air pollution, particularly NO_x (= NO + NO_2). Nitrogen-monoxide (NO) accounts for the majority of direct traffic emissions, which is subsequently oxidized to form NO_2 although some NO_2 is emitted directly (Ban-Weiss et al., 2008; Henderson et al., 2007; Kirchstetter et al., 1999). NO_2 levels are often strongly correlated with many other toxic air pollutants. Its concentration can be easily and precisely measured, which is helpful in assessing general air quality. Since it is a short-lived compound gas from numerous different sources, its concentrations can vary strongly, both in space and time.

According to the 2017 European Environment Agency report (EEA, 2017), some NO_2 concentrations measured at air quality monitoring stations are above the World Health Organization (WHO) Air Quality Guideline (AQG) values of $200\,\mu g/m^3$ (hourly) and $40\,\mu g/m^3$ (annually). $10.5\,\%$ of the stations across European cities exceeded the annual limits including several German cities. None of the exceedances were observed at rural background stations, but in urban or suburban stations. More specifically, $89\,\%$ of the exceeded values were observed at traffic stations. The 2016 air quality report by the German Environment Agency (Umweltbundesamt) (UBA, 2017) also pointed out that the air pollution in urban conurbations was primarily affected by traffic. In the 2015 technical report by the Bavarian environment agency (Landesamt für Umwelt, LfU) (LfU, 2015), the on-road NO_2 concentration limits were exceeded in most Bavarian cities from 2000 to 2014. In particular, the annual NO_2 level in Munich measured at Landshuter Allee station was more than twice of the annual NO_2 limit value of the WHO AQG of $40\,\mu g/m^3$.

With a growing focus on air pollution in the public attention, stationary monitoring networks have been established all over the world. Monitoring stations continuously measures different pollutants and while most stations follow defined rules in terms of measurement height and distance to traffic emissions, the question remains, how representative are those point measurements for the city wide air quality. According to a study of the spatial distribution of NO_2 in Hong Kong (Zhu et al., 2018), large differences between mobile measurements around the city and seven local monitoring stations were observed. In order to determine the representativeness of air quality monitoring stations, different measurement methods have to be combined. Most monitoring stations utilize the ChemiLuminescence (CL) technique for NO_x measurements. Thereby the NO_2 concentration is determined indirectly by calculating the difference between NO_x and NO concentrations. The concentration of oxidized odd-Nitrogen species (NO_y) is inevitably included as a small measurement error. Nevertheless, the CL technique has a good detection sensitivity that is given by its low background signal. This is because for initiating the fluorescence no light source

https://doi.org/10.5194/acp-2019-1198
Preprint. Discussion started: 9 March 2020

Atmospheric Chemistry and Physics Discussions

is required (Dunlea et al., 2007). In this study, we compared our CL and cavity-enhanced DOAS (CE DOAS) data to the local air quality stations and studied the diffusion rate of NO_2 in both vertical and horizontal directions from one of the stations.

For our study we utilized a combination of long-path DOAS (LP-DOAS) instrument and a CE DOAS, as well as a Cavity Attenuated Phase shift Spectroscopy (CAPS) instrument to determine the spatio-temporal variability of NO_2 concentrations in the central area of Munich, CE DOAS is a spectroscopic measurement technique that uses an optical resonator to fold the absorption path into into a resonator (Zhu et al., 2018; Min et al., 2016; Thalman and Volkamer, 2010; Platt et al., 2009; Washenfelder et al., 2008; Venables et al., 2006; Langridge et al., 2006). CAPS (Herbelin et al., 1980) is a spectroscopic detection technology, generally referred to cavity enhanced optical absorption, which has also been applied for the detection of atmospheric pollutants in many studies (Xie et al., 2019; Kundu et al., 2019; Ge et al., 2013; Kebabian et al., 2008, 2005a). The advantage of CE DOAS and CAPS is the fact that they are not sensitive to other reactive nitrogen oxides in the atmosphere like some other in-situ NO_2 monitoring techniques. They are both characterized by a compact setup and have no sensitivity loss during the operation. For mobile measurements a fast sampling rate is necessary, and the high accuracy of the instruments allowed a sampling rate of 2 s. Similar instrument setups have been used in many on-road studies of vehicles emissions (Zhu et al., 2018; Chan et al., 2017; Rakowska et al., 2014; Ning et al., 2012; Uhrner et al., 2007; Vogt et al., 2003).

In order to verify whether the LP DOAS measurements are representative for the whole city, NO_2 data from the Ozone Monitoring Instrument (OMI) on-board the NASA Aura satellite was used. Satellite measurements are commonly used for global scale long-term observation of aerosols and trace gases (Silvern et al., 2019; Zara et al., 2018; Laughner and Cohen, 2017; Inness et al., 2015). Validation studies revealed that satellite retrievals generally underestimate urban areas but also found good correlations between satellite and ground based observations (Chan et al., 2018; Lin et al., 2012; Lamsal et al., 2008; Wenig et al., 2008; Petritoli et al., 2004).

For our study we conducted on-road measurements of NO_2 concentrations in June and July of 2016 in order to investigate street level air quality and locate emission hot spot areas. Additionally, LP DOAS measurements were conducted to observe the temporal variability of ambient NO_2 in Munich. A measurement system consisting of several DOAS instruments was continuously operational for over 2 years (see Sec. 2). The algorithm that combines the mobile and stationary measurement data is described in Section 3.1.1. The resulting on-road NO_2 spatial patterns are presented in Section 3.1.2. The CE DOAS and CL were set up next to the Bavarian LfU local air quality station to measure the horizontal and vertical NO_2 distributions, and the results are shown in Section 3.2. In addition, Section 3.3 presents the comparison of LP DOAS NO_2 measurements with OMI satellite data, and analyzes the characteristics of seasonal NO_2 variation.

2 Methodology

This study combines different measurement methods such as mobile, stationary and satellite measurements to answer the question of how representative sparse point measurements are to determine the air quality of a city. Furthermore, we want to find out what kind of measurement approach is needed to determine the overall air quality in a city. The Munich three-dimensional DOAS measuring system combines three different types of DOAS instruments, specifically, CE DOAS and LP

https://doi.org/10.5194/acp-2019-1198
Preprint. Discussion started: 9 March 2020

Atmospheric Chemistry and Physics Discussions

DOAS. The measurement system is installed on the roof of the building of the Meteorological Institute Munich (MIM) at the Ludwig Maximilians University (LMU) in the center of Munich. The three LP DOAS instruments scan retro reflector arrays in different directions and distances, capturing the horizontal variations at the rooftop level. A CE DOAS is used to determine the NO_2 variability on the ground. The LP DOAS instruments run continuously, whereas the CE DOAS is used at different times of the year/week/day under varying meteorological conditions to determine street-level NO_2 distributions.

2.1 Mobile Measurements

A CE DOAS and a CAPS instruments in two vehicles were used for on-street sampling of traffic emissions. The sampling inlets were located at the front right window of each vehicle at $1.5\,\mathrm{m}$ height. For measurements in Munich's city park (English Garden), we used a bike trailer. The measurements were performed in June and July 2016 to cover a large part of the urban area in Munich. The sample resolution of the CE DOAS and the CAPS were both adjusted to $2\,\mathrm{s}$ during the mobile measurements. The measurements were performed on varying routes during daytime to cover the entire city center area.

The CE DOAS is composed of an air sampling system, an optical resonator with two high reflective mirrors, a blue LED light source and a spectrometer (Platt et al., 2009). For the spectral retrieval in the wavelength range $435.6\,\mathrm{nm}$ to $455.1\,\mathrm{nm}$, we used DOASIS (Kraus, 2005). The NO_2 reference absorption cross is from Vandaele et al. (2002), O_4 from Hermans et al. (1999), H_2O from Rothman et al. (2003) and CHOCHO (Glyoxal) from Volkamer et al. (2005).

The CAPS measurement technique is closely related to Cavity Ring-Down Laser absorption Spectroscopy (CRDS), which determines the concentration of trace gases from the decay rate of the light source in the optical resonator (Ball and Jones, 2003; Brown et al., 2002; Berden et al., 2000; Engeln et al., 1996). CRDS is a laser-based system, while CAPS uses an incoherent light source (a blue LED) that is well-matched to the NO_2 absorption band. The CAPS NO_2 system mainly consists of a blue LED, a measurement chamber with two highly reflective mirrors centered at $450\,\mathrm{nm}$, and a vacuum photodiode detector. It estimates the NO_2 concentration by directly measuring the optical absorption of NO_2 at the $450\,\mathrm{nm}$ wavelength within the electromagnetic spectrum. The light appears as a distorted waveform after passing through two mirrors and the measurement cell, which is characterized by a phase shift that is determined by demodulation techniques in comparison to the initial LED light modulation. The phase shift is proportional to the absorbance of the light by the presence of NO_2. The concentration of NO_2 can be derived by measuring the amount of the phase shift. The detailed principles of the CAPS system are demonstrated in Kebabian et al. (2008, 2005b).

2.2 Long-path (LP) DOAS observations

Three LP DOAS instruments were installed on the roof of the MIM. The measurement setups are displayed in Figure 1. The measurement system started operation in December 2015 with a total absorption path of $3828\,\mathrm{m}$ across the English Garden to a retro reflector array located on the rooftop of the Hilton hotel building at $\sim 48\,\mathrm{m}$ height. In January 2017 another absorption path of $1142\,\mathrm{m}$ was installed covering three blocks around the university area to a retro reflector at the St. Ludwig Munich Church at $\sim 40\,\mathrm{m}$ above ground. Since July 2015 a retro reflector is also installed at the roof of the N5 building of the Technical University of Munich (TUM) at $\sim 28\,\mathrm{m}$ height, allowing an absorption path of $828\,\mathrm{m}$. From July 2016 to August 2017 a path of

https://doi.org/10.5194/acp-2019-1198
Preprint. Discussion started: 9 March 2020

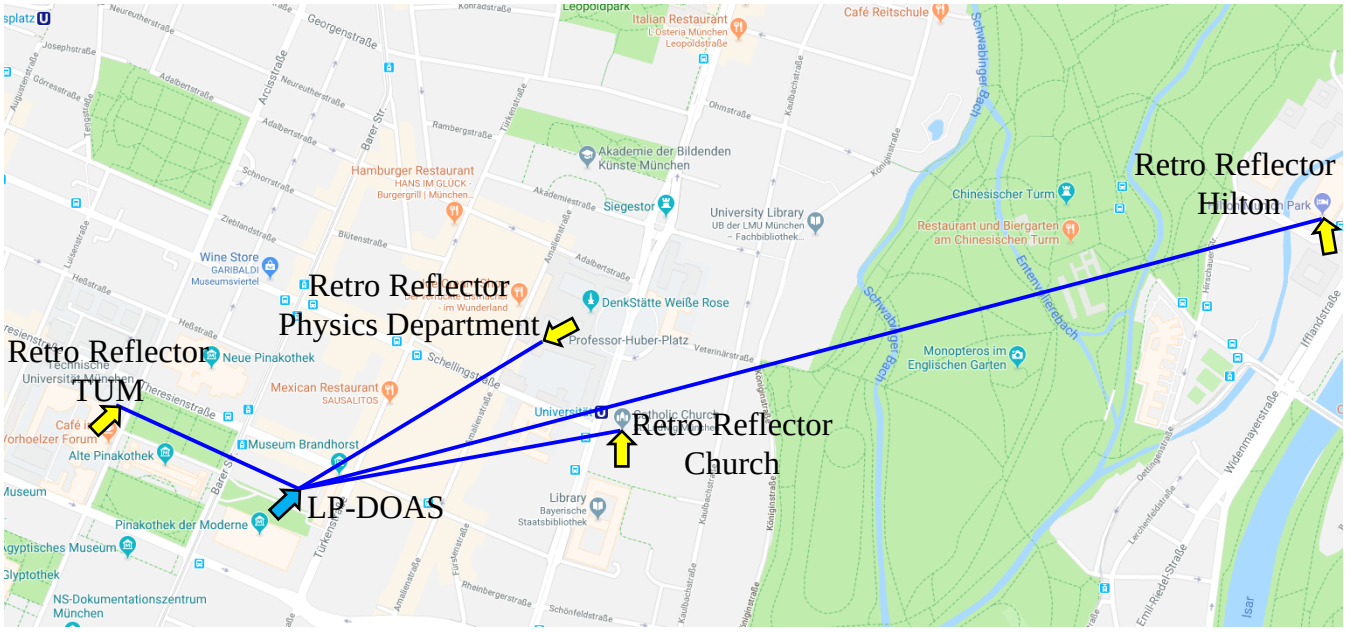

Figure 1. Map of Munich city center and four optical paths of three LP DOAS instruments. Map data ©Google maps.

816 m to the roof of the building of the Physics department of LMU at ∼24 m height was operational as well. The measurement paths cover the university campus, the public park, residential areas and areas with heavy traffic. The instrumental background was corrected by subtracting the LED reference spectra, including dark current, offset, and background, from each measured spectrum.

A measurement sequence starts by taking a LED reference spectra using a shortcut system consisting of a diffuser plate in front of the y-fiber and an exposure time of 10 s. Then a shutter is used to block the LED for measuring the atmospheric background spectrum for 1 s. Afterwards, the atmospheric spectrum with a maximum of 10 scans is taken. Each scan of a spectrum has a peak intensity of about 60 % to 80 % saturation of the detector and typically requires 60 ms to 1000 ms, depending on the visibility and instrument setup. The total sampling time (the product of the number of scans and exposure time for each scan) was limited to 60 s. A full measurement sequence took between 30 s and 90 s, depending on visibility conditions.

2.3 Local air quality monitoring network

The Bavarian LfU is operating five monitoring stations, three roadside stations at Landshuter Allee, Stachus and Lothstrasse, and two ambient stations in Allach and Johanneskirchen. In these stations the air pollutants NO, NO_2, CO, O_3, $PM_{2.5}$, PM_{10} and in addition meteorological parameters such as relative humidity and temperature are measured. In this study we con-

https://doi.org/10.5194/acp-2019-1198
Preprint. Discussion started: 9 March 2020

Atmospheric Chemistry and Physics Discussions

centrated on the NO and NO_2 concentrations that are continuously monitored using an in situ CL NO_x analyzer (HORIBA APNA-370) (LfU, 2019).

2.4 The Ozone Monitoring Instrument (OMI) satellite observations

The Ozone Monitoring Instrument (OMI) is an imaging spectrometer on board the NASA Aura satellite. It measures earthshine radiances with two grating spectrometers which cover the wavelength range from $264\,\mathrm{nm}$ to $504\,\mathrm{nm}$. OMI provides the daily measurements of NO_2, BrO, SO_2, O_3, HCHO, OClO, BrO and aerosols in a global coverage. It is able to detect the cloud radiance fraction, cloud pressure and albedo.

NASA's OMI standard product version 3 (SPv3) (Krotkov et al., 2017; Marchenko et al., 2015) is used in this study. The OMI NO_2 data is publicly available at the Goddard Earth Sciences Data and Information Services Center (GES DISC) (https://disc.gsfc.nasa.gov/). For our comparison we gridded the OMI VCDs onto a high resolution grid with $0.02° \times 0.02°$ following the approach described in previous studies (Chan et al., 2015; Kuhlmann et al., 2014).

2.4.1 Converting OMI vertical column densities to ground mixing ratio using modeled NO_2 profiles

In order to examine how representative the LP DOAS data is for the temporal pattern observed by OMI, which covers the entire city, OMI's vertical column densities (VCDs) are converted into ground concentrations. For the conversion, vertical profile information is needed. We utilized NO_2 vertical profile information simulated by the chemistry transport model (CTM) GEOS-Chem (Bey et al., 2001). The horizontal resolution of the simulation is $2.0°$ (latitude) $\times$ $2.5°$. Vertical profiles of NO_2 are spatially interpolated within the 4 closest grid cell to the measurement location. Detailed description of the GEOS-Chem simulation can be found in previous studies (Chan, 2017a, b).

Since we use the LP DOAS data for the diurnal correction, we tested the correlation between LP DOAS measurement values and OMI data. The OMI satellite measurements cover a larger area of Munich with the instrument's ground pixel footprint of $\sim$320 - 6400 km^2 than the $2\,\mathrm{km}$ path length of the LP DOAS instrument. A good correlation would allow the assumption that the relative diurnal cycle obtained from the LP DOAS can be regarded as being representative for the entire urban area.

3 Results and Discussion

3.1 NO_2 concentration maps constructed using mobile measurements

The mobile measurement data can be used to create a map showing the city-wide distribution of air quality using NO_2 concentrations as a general indicator (Figure 3). As a first test, we compared the averaged measurement values within a $10\,\mathrm{km}$ radius around the three governmental monitoring stations at Landshuter Allee, Lothstrasse and Stachus and obtained an averaged concentration of $93\,\mu\mathrm{g}/\mathrm{m}^3$ for the mobile measurements and $48\,\mu\mathrm{g}/\mathrm{m}^3$ for the three stations for the campaign days in June and July 2016. The large difference can be explained by looking at the criteria for the location of monitoring sites set by the European Union: the recommended measurement height is between $1.5\,\mathrm{m}$ and $4\,\mathrm{m}$, maximum distance to the street is $10\,\mathrm{m}$

https://doi.org/10.5194/acp-2019-1198
Preprint. Discussion started: 9 March 2020

Atmospheric Chemistry and Physics Discussions

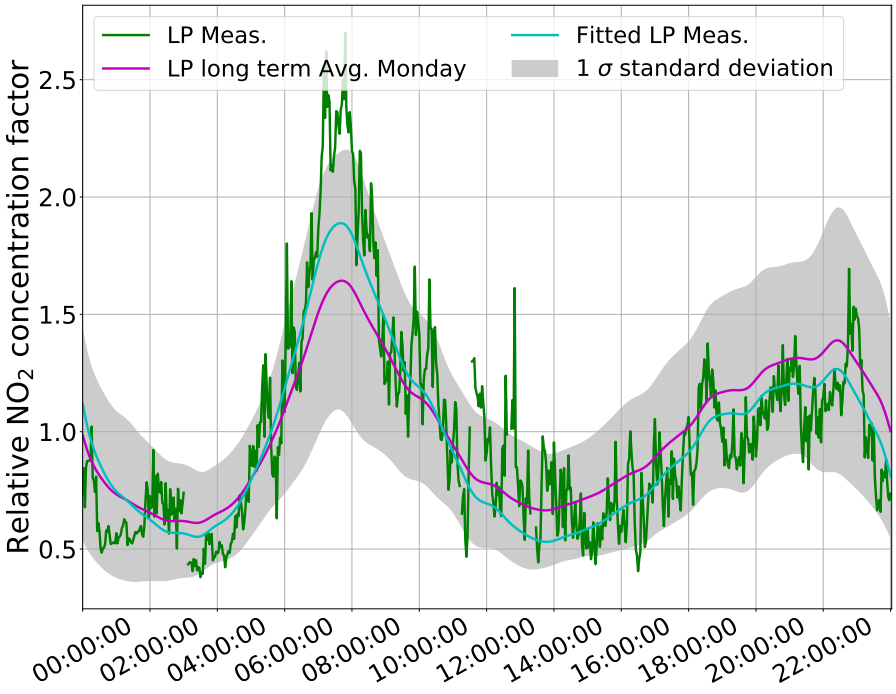

Figure 2. Normalization curve used to correct mobile measurement data. The purple curve is the long term average diurnal pattern for the day of the week of the measurement day (Monday in this example), which is fitted (scaling with linear time dependent factor and offset) to the measurement data of 13^{th} June 2016 shown in green, excluding the data outside of the $2\,\sigma$ area shown in gray. The resulting cyan curve is used to remove the diurnal dependency of the mobile measurements data.

and at a minimum distance to the next crossroad of $25\,\mathrm{m}$ (Commission, 2008). Most monitoring stations have the inlet positioned at $4\,\mathrm{m}$ height. The mobile measurement data, however, include the significantly increased concentrations at crossroads, tunnel exits and other pollution hot spots. In addition, the height of the measurement inlets differs by $2.5\,\mathrm{m}$ between the mobile measurements and the governmental monitoring stations, which also influences the comparison. In order to determine how representative point measurements are for the city-wide air quality, we analyzed the correlation between point measurements and the distribution captured by mobile measurements, between point and path averaging measurements, and between path averaging and satellite measurements. Since the spatial distribution can not be captured instantaneous, an algorithm to normalize for the diurnal variation is needed in order to create a consistent map representing only the spatial variability of daily average concentrations instead of temporal influences.

https://doi.org/10.5194/acp-2019-1198
Preprint. Discussion started: 9 March 2020

Atmospheric Chemistry and Physics Discussions

3.1.1 Normalization of the diurnal cycle

As a mobile survey cannot capture the concentrations at different locations simultaneously, and the NO_2 measurements are naturally influenced by daily variations such as changing boundary layer height or the diurnal cycle of the traffic amount, we use an algorithm to separate temporal and spatial patterns in the data set.

First, the algorithm normalizes the long time series of LP DOAS measurements of atmospheric NO_2 by dividing through the daily average NO_2 concentration of the same day. The mean concentration curves for each day of the week over a period of 2.5 years are calculated in order to obtain a relative diurnal NO_2 variation pattern (purple curve in Figure 2). The normalized averaged diurnal NO_2 curve of the corresponding weekday is fitted (using an offset and a scaling with a linearly time dependent factor) to the normalized LP DOAS measurement of the corresponding day, coinciding with the mobile measurements. In order to remove the influence of outliers, NO_2 values outside of $2\,\sigma$ variation of the fitted curve are disregarded (cyan curve). Figure 2 shows the fitting process for the normalization curve for one day of the measurement campaign. The other days show very similar characteristics with a significant peak in the morning and evening rush hours. Dividing the mobile measurement data by the curve data, removes the diurnal dependencies and allows focusing on spatial pattern.

3.1.2 Spatial distribution of NO_2 in the city of Munich

The measured concentrations during the campaign were spatially averaged to a high resolution grid of $20\,\mathrm{m} \times 20\,\mathrm{m}$ (Figure 3a). Most of these measurements are distributed on major roads, including city, urban ring-road, suburbs, rural areas, and highways. Relatively high NO_2 pollution could be observed on motorways and busy urban roads. Difference between main roads and adjoining side roads of up to a factor of 5 can be observed. $4.4\,\%$ of the on-road measurements exceeded the WHO 1-hour guideline value of $200\,\mu\mathrm{g/m^3} \approx 106\,\mathrm{ppb}$ (depending on temperature, here the appropriate conversion factor at $25\,^{\circ}\mathrm{C}$ and $1013\,\mathrm{hPa}$ are used), corresponding to $6.6\,\%$ of the area covered. High NO_2 values over motorways were mainly due to the emission of heavy duty diesel vehicles, i.e. a significant increase could be observed when we were driving behind trucks and buses. In the city center traffic congestion and the street canyon effect (Rakowska et al., 2014) can be the main cause of elevated on-road NO_2 levels. Zhu et al. (2018) showed in a study in Hong Kong that average pollution exposure increases by $14.5\,\%$ when stopping at a traffic light compared to fluent traffic. Other studies showed as well that the distribution of pollutants is mainly impacted by traffic flow patterns (Fu et al., 2017; Rakowska et al., 2014; Huan and Kebin, 2012; Kaur et al., 2007; Westerdahl et al., 2005). The normalization using coinciding LP DOAS measurement removes the diurnal dependency but leaves the traffic flow dependency in the data, because it contributes to the city-wide air quality. The normalized on-road NO_2 map shown in Figure 3(b) represents daily average values for all locations. After normalization, there exist some regions, where NO_2 concentrations are consistently higher, while in other areas the normalized concentrations are lower than the original measurements. This behavior can be explained by the time of the day when the measurements were taken: when we measured during the rush hour, the measurements are higher, while the measurements during noon are lower than the daily average. The normalization procedure increased the occurrences of WHO 1-hour guideline exceedances to $14.5\,\%$ of the on-road measurements, corresponding to $17.1\,\%$ of the total area (including motorways) and $15.7\,\%$ of the area in the city center.

https://doi.org/10.5194/acp-2019-1198
Preprint. Discussion started: 9 March 2020

Atmospheric Chemistry and Physics Discussions

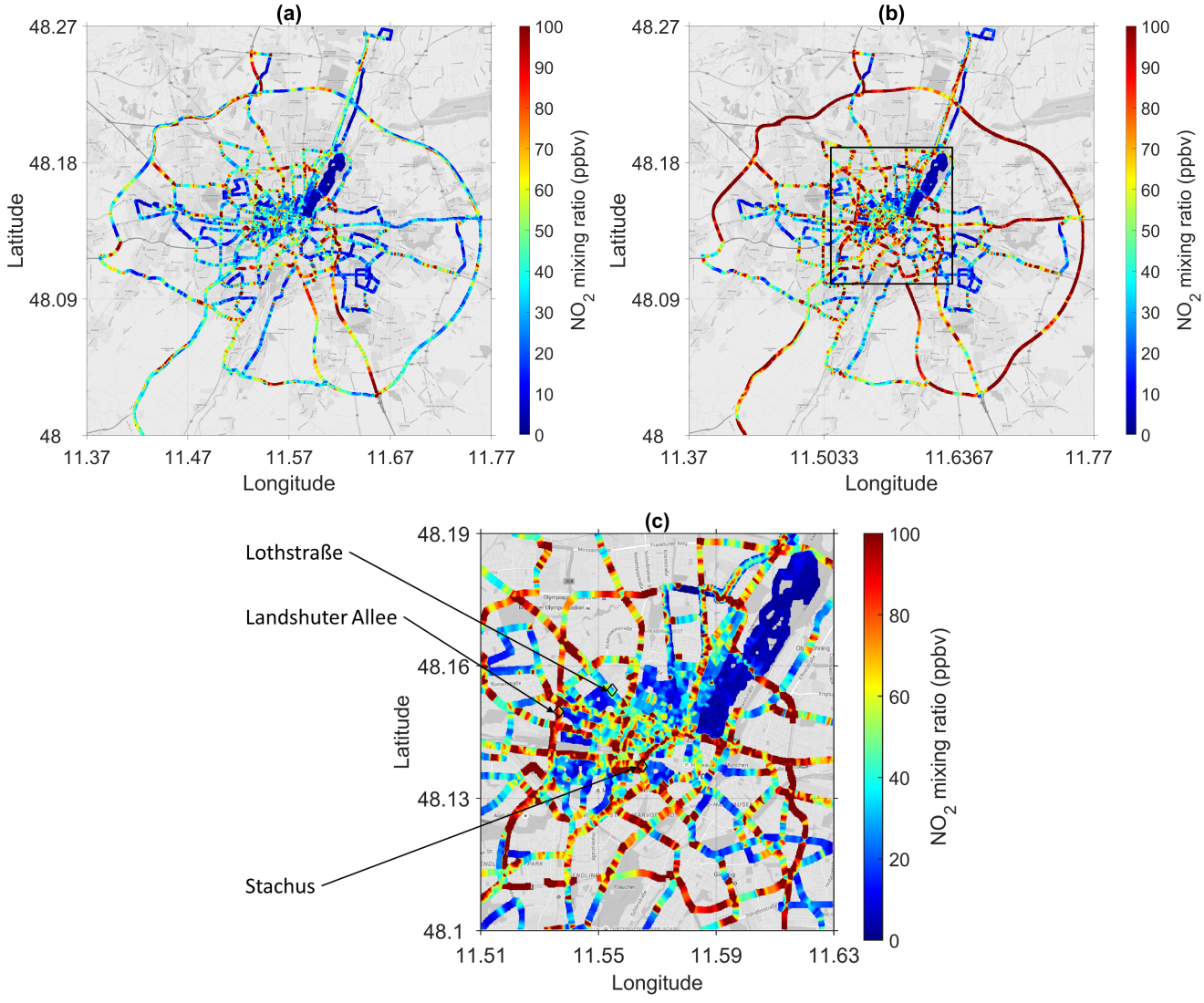

Figure 3. (a) CE DOAS and CAPS mobile measurements of NO_2 in Munich in 2016. (b) Normalized spatial distribution of NO_2 using coinciding LP DOAS data to remove the diurnal dependencies. (c) Zoom in of the city center. The three black diamonds in (c) are the locations of the governmental monitoring stations (Landshuter Allee, Lothstraße, Stachus). The area at the top right with very low concentrations represents the city park English Garden. Map data ©Google maps.

However, the thresholds in WHO AQG are based on studies involving monitoring station data which are not measuring directly on the street. Taking the vertical and horizontal dilution factors (see Figure 4, the factor 0.84 for $4\,\mathrm{m}$ height and 0.87 for $6\,\mathrm{m}$ distance) into account, we extrapolate WHO AQG 1-hour threshold value of $200\,\mu\mathrm{g/m^3}$ to the on-road level with the value of $273.7\,\mu\mathrm{g/m^3} \approx 145.6\,\mathrm{ppb}$ ($200\,\mu\mathrm{g/m^3}/0.84/0.87$)), then also calculated the frequency of exceedances (cf. table 1).

https://doi.org/10.5194/acp-2019-1198
Preprint. Discussion started: 9 March 2020

Atmospheric Chemistry and Physics Discussions

Table 1. Percentage of measured concentrations exceeding the WHO AQG and its corrected on-road level thresholds for both temporal and spatial coverage. The values are broken down for before and after the normalization of the data according to diurnal patterns, and also calculated for WHO guideline values adjusted for the different measurement height and distance to the street.

	Percentage exceeding WHO guideline		Percentage exceeding adjusted WHO guideline	
	Before normalization	After normalization	Before normalization	After normalization
Temporally	4.4 %	14.5 %	1.7 %	6.7 %
Spatially (total)	4.1 %	17.1 %	1.1 %	4.6 %
Spatially (downtown)	5.5 %	12.4 %	1.6 %	4.7 %

It can be seen that especially in the downtown area (Figure 3c), the values after the normalization are noticeable higher than before. This can be explained as we tried to avoid the rush hours, i.e. traffic jams, for performing the measurements. Therefore, the measured NO_2 level is often lower in comparison to the day-average. The area with significantly lower concentrations seen in Figure 3 is the city park (English Garden) with no vehicle emissions and where plants could provide deposition areas for O_3 , NO_x and particles (Chaparro-Suarez et al., 2011; Wesely and Hicks, 2000).

3.2 Comparison of NO_2 concentrations at different heights and distances from the street

In order to investigate the diffusion effects of emitted NO_2 molecules in both vertical and horizontal directions, measurements were conducted over two days (20th. and 22th. March 2019) using CE DOAS and CL instruments at Stachus, Munich, next to the governmental monitoring station. Since we used two different measurement techniques, the first step was to check the instrument for consistency. Side-by-side measurements next to the street (same height and distance to the street in Figure 4) were used to analyze differences. We found the CL NO_2 to be $2\,\%$ higher, possible due to sensitivities of the molybdenum oxide converters to NO_y species (see Villena et al., 2012; Dunlea et al., 2007). We corrected the CL measurement data in order to remove those interferences.

Both instruments were set up next to the governmental monitoring station at Stachus, which is at a height of $4\,\mathrm{m}$ and has a $30\,\mathrm{min}$ time resolution. The CE DOAS was set up next to the street and measured at a fixed height of $1.5\,\mathrm{m}$ above the ground, while the CL instrument measured NO_2 at multiple heights above the ground (from $0.5\,\mathrm{m}$ to $4\,\mathrm{m}$) and at different distances from the side of the street (from $2\,\mathrm{m}$ to $10\,\mathrm{m}$). The temporal resolution for both instruments was set to $5\,\mathrm{s}$. All measurements are shown in Figure 4(a) for the different measurement heights and (b) for the different distances to the side of the street. Figure 4(c) shows the distribution of the ratios, and it can clearly be seen that the average concentrations decrease with height and distance. Figure 4(d) shows a two-day comparison between the $30\,\mathrm{min}$ average NO_2 concentrations measured with our CE DOAS at a height of $1.5\,\mathrm{m}$ with the CL instrument data of the governmental monitoring station at a height of $4\,\mathrm{m}$. The regression plot shows a ratio of 1.23 between the measurements at $1.5\,\mathrm{m}$ and $4\,\mathrm{m}$ height. We repeated the $1.5\,\mathrm{m}$ to $4\,\mathrm{m}$ measurement height comparison on several different days at different seasons and derived the same factor of 0.84 with

https://doi.org/10.5194/acp-2019-1198
Preprint. Discussion started: 9 March 2020

Atmospheric Chemistry and Physics Discussions

a standard deviation of 0.21, so most ratios vary from 37 % decrease with increasing height (factor 0.84-0.21=0.63) to 5 % increase (factor 0.84+0.21)=1.05). Since the inlet height for our mobile measurements is 1.5 m, we take this factor into account when comparing to monitoring station data. In terms of distance to the street, measuring at the center of the street, like we did during the mobile measurements, and measuring at a distance of 6 m, which is approximately the distance of most monitoring stations to the middle of the street, the on-road measurements are 13 % higher due to the observed diffusion effects. Those factors have to be kept in mind when comparing on-road measurements to monitoring station data or any other measurement data taken at different height levels and distances to the street. This leads to the conclusion, that from the 48 % difference between the average concentrations of three monitoring stations ($48\,\mu g/m^3$) and the mobile measurements around the three stations ($93\,\mu g/m^3$), both averaged for the measurement campaign period, 27 % can be explained by the difference in inlet height and distance to the street, and the remaining 21 % is due to the fact, that the monitoring stations are positioned away from pollution hot spots at crossroads according to WHO guidelines.

3.3 Comparison between ground measurement and converted OMI observation

Satellite measurements are strongly affected by clouds, as clouds shield ground level NO_2. Hence, to compare with the LP DOAS data, OMI data with cloud fractions larger than 50 %, which were significantly influenced by clouds, were filtered out. LP DOAS data from 12:00 - 15:00 UTC, same as the OMI overpass time for Munich, were used for comparing with the average OMI data sets within 10 km and 50 km from the measurement site (Figure 5). To reduce the impact of clouds and local spatial variations, we use monthly average data to compare. The uncertainty of the LP DOAS measurements, which was smaller than 1 ppb for a single measurement, is too small to be shown for monthly averages so the standard deviation within each month is shown in Figure 5. Observation of LP DOAS and OMI both showed a similar annual trends, with higher NO_2 levels in winter and lower NO_2 levels in summer.

Comparing monthly means of LP DOAS overpass time measurements with OMI retrieved ground mixing ratios of NO_2 and VCDs within 10 km show correlation coefficients of 0.85 and 0.72, respectively (Figure 6). OMI and the corresponding overpass time measurements of LP DOAS correlate well, indicating OMI measured reliable tendency of ground level NO_2. The discrepancy of correlation coefficients were mainly caused by the vertical profile used for the OMI retrieval and the conversion of VCDs to ground level mixing ratios. In order to show the influence of temporal averaging and assess the temporal representativeness of the governmental monitoring station data, monthly averages for all LP DOAS data and the data of three governmental monitoring stations are shown in Figure 5 as well. In addition, the data of the governmental monitoring stations were 15.4 ppb on average higher than the LP DOAS measurements. The Pearson correlation between the two data sets was 0.32. The low correlation may be due to the different measurement areas, measurement heights and measurement resolution.

Average variability of the NO_2 mixing ratios in winter (November to February) and summer (June to August) were 16.5 ppb and 5.5 ppb. The errors bars of OMI data do not overlap with the LP DOAS data for most months, neither within 10 km nor within 50 km, which demonstrated that there might be systematic errors in the conversion of VCDs to ground level mixing ratios or in the OMI retrieval process itself (Wenig et al., 2008). As the previous study also suggests, lower OMI values over cities compared to ground measurements could be due to the OMI a-priori profile used for both, the VCD retrieval and

https://doi.org/10.5194/acp-2019-1198
Preprint. Discussion started: 9 March 2020

Atmospheric Chemistry and Physics Discussions

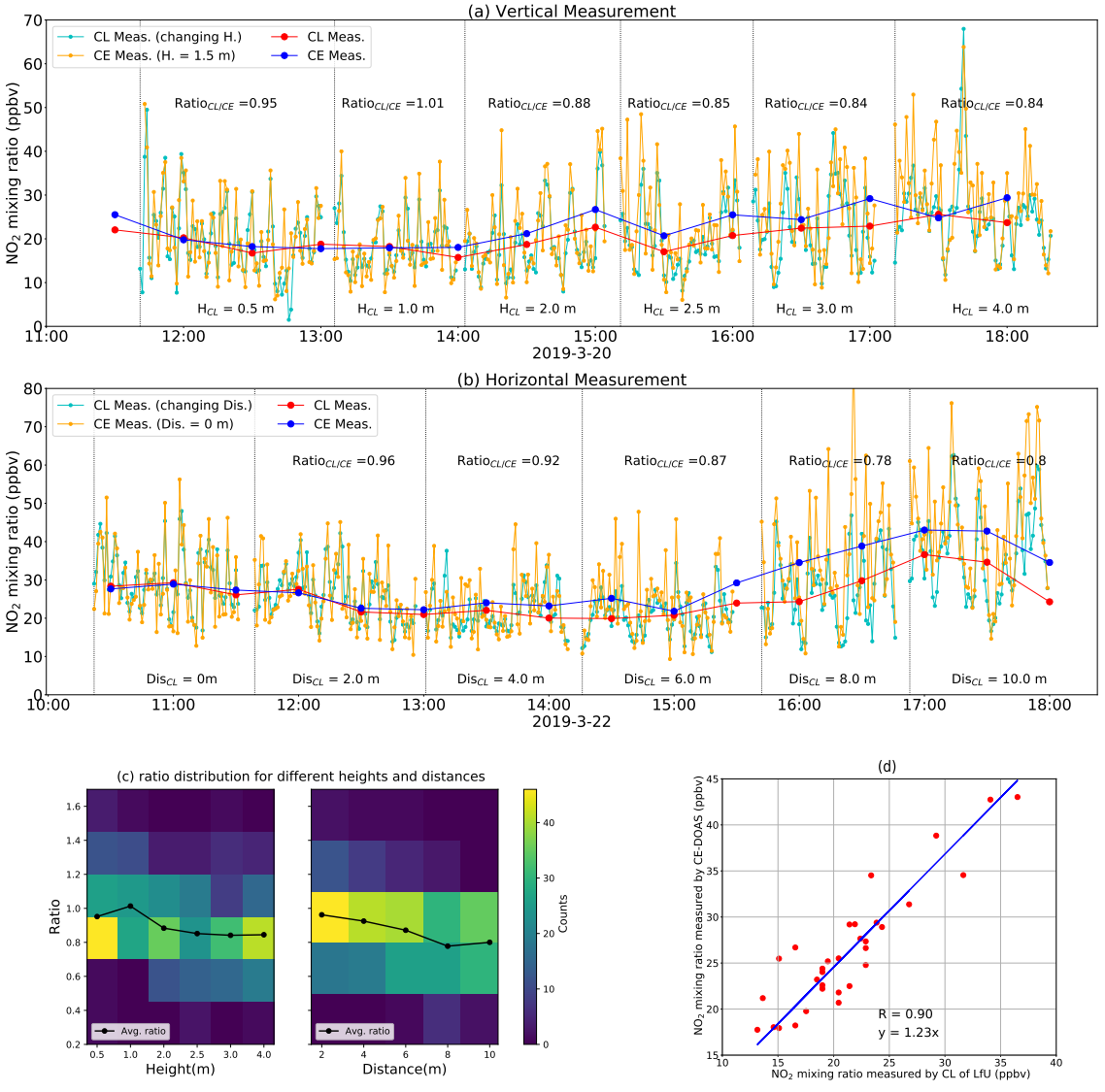

Figure 4. NO_2 measurements at Karlsplatz (Stachus), Munich, with different heights above ground (a) and distances to the main street (b). The ratio between 1-minute averaged CE DOAS and coinciding CL measurements were calculated individually for the different heights and distances. Half-hour averaged CE DOAS measurements (blue curve) were compared with the corresponding CL measurements (red curve). Averaged ratios for different heights and distances (as defined in (a)) are shown in (c), CE DOAS measurements at 1.5 m were averaged to 30 min intervals and compared with the half-hourly data of the governmental monitoring station at 4 m shown in (d)

https://doi.org/10.5194/acp-2019-1198
Preprint. Discussion started: 9 March 2020

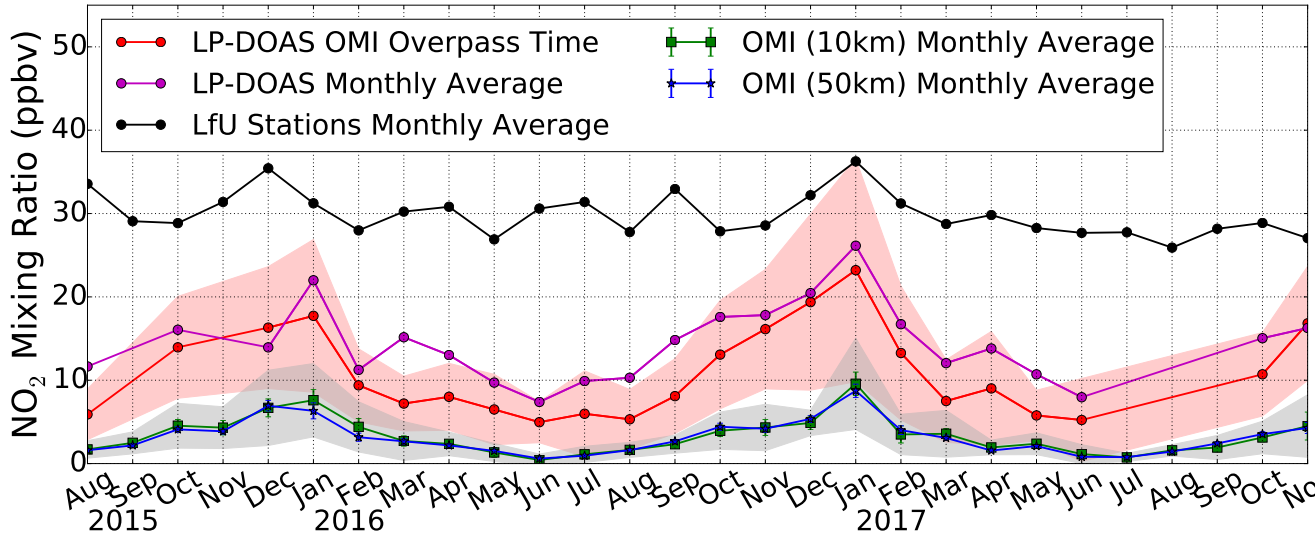

Figure 5. Monthly average ground-level NO_2 mixing ratio. The monthly average NO_2 of the governmental monitoring stations (Landshuter Allee, Lothstraße, Stachus) is shown. LP DOAS data are temporal averages around OMI overpass time (12:30 – 14:30 UTC). OMI data are spatial averages over pixels within a 10 km and 50 km radius of our institute. The red shadow indicate the variability of 1 σ (standard deviation) of averaged LP DOAS measurements of OMI overpass time. The light gray regions indicate 1 σ variability of OMI data within 10 km

converting the tropospheric NO_2 VCDs to ground level mixing ratios, was taking an average over a larger area, not only urban areas, but also rural areas with a lower ground level mixing ratio to total column ratios. A total underestimation for the ground level NO_2 of about 69 % can be observed. A similar result was found by Kuhlmann et al. (2015). However, because of the good correlation it is safe to assume that relative temporal changes captured by the LP DOAS can be regarded as representative for area covered by OMI that spans the entire city of Munich.

4 Summary and conclusions

Mobile road measurements using CE DOAS and CAPS instruments combined with an algorithm for correcting the diurnal cycle were used in order to generate a consistent pollution map of the street level NO_2 concentration in Munich. This map is not only used to identify pollution hot spots but also to figure out how representative the existing NO_2 point measurements are for the whole city. Elevated NO_2 levels can be observed mostly on motorways and busy city roads, due to the emission of heavy duty vehicles or heavy traffic volume. When averaging the mobile measurements around the monitoring stations, we derived an average NO_2 concentration of 93 $\mu g/m^3$, whereas the three monitoring stations at the city center reported 48 $\mu g/m^3$ on average for the same time, so 48 % lower values. Our analysis shows that the different measurement height can account for 16 % difference (factor 0.84), and the distance of the sample inlets to the center of the street, where the mobile measurements took

https://doi.org/10.5194/acp-2019-1198
Preprint. Discussion started: 9 March 2020

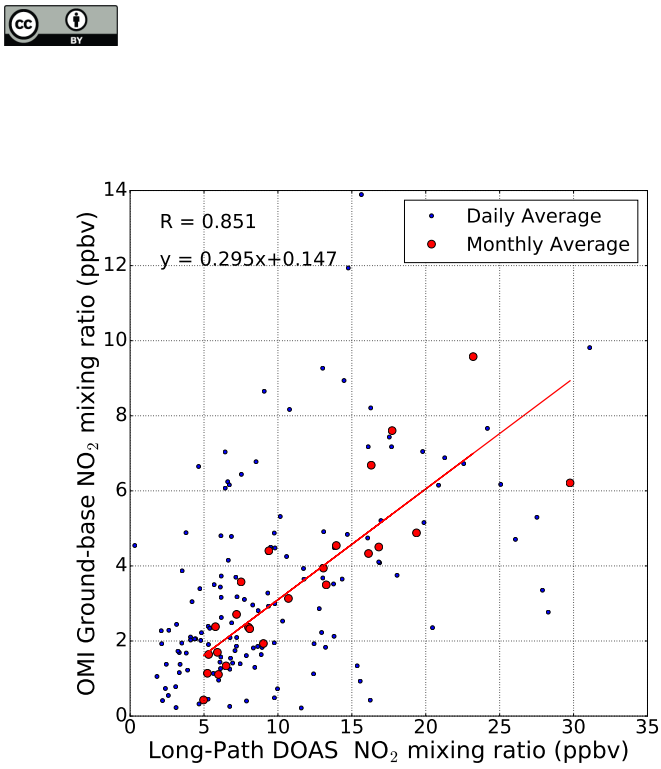

Figure 6. Correlation of LP DOAS measurements with retrieved NO_2 mixing ratio (ppbv) in (a) and VCD in (b) of OMI observation.

place explains the 13 % (factor 0.87) lower values. Accounting for these factors still leaves about 21 % that can be attributed to pollution hot spots like busy cross roads or tunnel exits. These hot spots are not covered by monitoring stations which is intentionally done in order to make the long term data less dependent on local events. Nevertheless, the differences observed in the presented study shows that point measurements are likely not representative for the NO_2 concentration in the whole city. Most network measurement sites are not capturing the concentrations people are exposed to when walking or driving at street level but are instead focusing on long term trends. Our study illustrates the importance of combining different measurement techniques to capture spatial and temporal patterns within a city and derive concentration values that are representative for the air most people breathe in.

The pollution maps generated in this project provide valuable information for future urban planning and the design of control measures of environment pollution. Furthermore, it can provide guidelines for identifying representative locations for air pollution monitoring stations in a city. Additionally, the observed spatial distribution of NO_2 concentrations are also beneficial to the validation of chemical transport models and assessment studies of the impact of air pollution on human health.

Author contributions. YZ, MW and JC designed the experiments. YZ, GK and XB carried them out. KLC simulate the results from GEOS-Chem model. YZ prepared the manuscript with contributions from all co-authors.

https://doi.org/10.5194/acp-2019-1198
Preprint. Discussion started: 9 March 2020

Atmospheric Chemistry and Physics Discussions

Competing interests. The authors declare that they have no conflict of interest.

Acknowledgements. The work described in this paper was jountly supported by the major research instrumentation programme INST 86/1499 FUGG.

https://doi.org/10.5194/acp-2019-1198
Preprint. Discussion started: 9 March 2020

Atmospheric Chemistry and Physics Discussions

References

Ball, S. M. and Jones, R. L.: Broad-band cavity ring-down spectroscopy, Chemical reviews, 103, 5239–5262, 2003.

Ban-Weiss, G. A., McLaughlin, J. P., Harley, R. A., Lunden, M. M., Kirchstetter, T. W., Kean, A. J., Strawa, A. W., Stevenson, E. D., and Kendall, G. R.: Long-term changes in emissions of nitrogen oxides and particulate matter from on-road gasoline and diesel vehicles, Atmospheric Environment, 42, 220–232, 2008.

Berden, G., Peeters, R., and Meijer, G.: Cavity ring-down spectroscopy: Experimental schemes and applications, International Reviews in Physical Chemistry, 19, 565–607, 2000.

Bey, I., Jacob, D. J., Yantosca, R. M., Logan, J. A., Field, B. D., Fiore, A. M., Li, Q., Liu, H. Y., Mickley, L. J., and Schultz, M. G.: Global modeling of tropospheric chemistry with assimilated meteorology: Model description and evaluation, Journal of Geophysical Research: Atmospheres, 106, 23 073–23 095, https://doi.org/10.1029/2001JD000807, 2001.

Brown, S., Stark, H., and Ravishankara, A.: Cavity ring-down spectroscopy for atmospheric trace gas detection: application to the nitrate radical (NO 3), Applied Physics B, 75, 173–182, 2002.

Chan, K.: Aerosol optical depths and their contributing sources in Taiwan, Atmospheric environment, 148, 364–375, 2017a.

Chan, K.: Biomass burning sources and their contributions to the local air quality in Hong Kong, Science of the Total Environment, 596, 212–221, 2017b.

Chan, K., Hartl, A., Lam, Y., Xie, P., Liu, W., Cheung, H., Lampel, J., Pöhler, D., Li, A., Xu, J., et al.: Observations of tropospheric NO2 using ground based MAX-DOAS and OMI measurements during the Shanghai World Expo 2010, Atmospheric Environment, 119, 45–58, 2015.

Chan, K., Wiegner, M., Wenig, M., and Pöhler, D.: Observations of tropospheric aerosols and NO_2 in Hong Kong over 5years using ground based MAX-DOAS, Science of The Total Environment, 619-620, 1545–1556, https://doi.org/10.1016/j.scitotenv.2017.10.153, 2018.

Chan, K. L., Wang, S., Liu, C., Zhou, B., Wenig, M. O., and Saiz-Lopez, A.: On the summertime air quality and related photochemical processes in the megacity Shanghai, China, Science of The Total Environment, 580, 974–983, https://doi.org/http://dx.doi.org/10.1016/j.scitotenv.2016.12.052, 2017.

Chaparro-Suarez, I., Meixner, F., and Kesselmeier, J.: Nitrogen dioxide (NO2) uptake by vegetation controlled by atmospheric concentrations and plant stomatal aperture, Atmospheric Environment, 45, 5742 – 5750, https://doi.org/https://doi.org/10.1016/j.atmosenv.2011.07.021, http://www.sciencedirect.com/science/article/pii/S1352231011007461, 2011.

Commission, E.: Directive 2008/50/EC of the European Parliament and of the Council of 21 May 2008 on ambient air quality and cleaner air for Europe, Official Journal of the European Union, 2008.

Dunlea, E. J., Herndon, S. C., Nelson, D. D., Volkamer, R. M., San Martini, F., Sheehy, P. M., Zahniser, M. S., Shorter, J. H., Wormhoudt, J. C., Lamb, B. K., Allwine, E. J., Gaffney, J. S., Marley, N. A., Grutter, M., Marquez, C., Blanco, S., Cardenas, B., Retama, A., Ramos Villegas, C. R., Kolb, C. E., Molina, L. T., and Molina, M. J.: Evaluation of nitrogen dioxide chemiluminescence monitors in a polluted urban environment, Atmospheric Chemistry and Physics, 7, 2691–2704, https://doi.org/10.5194/acp-7-2691-2007, 2007.

EEA: Air quality in Europe–2017 Report, Tech. rep., European Environment Agency Copenhagen, Denmark, 2017.

Engeln, R., von Helden, G., Berden, G., and Meijer, G.: Phase shift cavity ring down absorption spectroscopy, Chemical Physics Letters, 262, 105 – 109, https://doi.org/https://doi.org/10.1016/0009-2614(96)01048-2, http://www.sciencedirect.com/science/article/pii/0009261496010482, 1996.

https://doi.org/10.5194/acp-2019-1198
Preprint. Discussion started: 9 March 2020

Fu, X., Liu, J., Ban-Weiss, G. A., Zhang, J., Huang, X., Ouyang, B., Popoola, O., and Tao, S.: Effects of canyon geometry on the distribution of traffic-related air pollution in a large urban area: Implications of a multi-canyon air pollution dispersion model, Atmospheric Environment, 165, 111–121, https://doi.org/10.1016/j.atmosenv.2017.06.031, http://www.sciencedirect.com/science/article/pii/S1352231017304120, 2017.

Ge, B., Sun, Y., Liu, Y., Dong, H., Ji, D., Jiang, Q., Li, J., and Wang, Z.: Nitrogen dioxide measurement by cavity attenuated phase shift spectroscopy (CAPS) and implications in ozone production efficiency and nitrate formation in Beijing, China, Journal of Geophysical Research: Atmospheres, 118, 9499–9509, 2013.

Henderson, S. B., Beckerman, B., Jerrett, M., and Brauer, M.: Application of land use regression to estimate long-term concentrations of traffic-related nitrogen oxides and fine particulate matter, Environmental science & technology, 41, 2422–2428, 2007.

Herbelin, J. M., McKay, J. A., Kwok, M. A., Ueunten, R. H., Urevig, D. S., Spencer, D. J., and Benard, D. J.: Sensitive measurement of photon lifetime and true reflectances in an optical cavity by a phase-shift method, Appl. Opt., 19, 144–147, https://doi.org/10.1364/AO.19.000144, http://ao.osa.org/abstract.cfm?URI=ao-19-1-144, 1980.

Hermans, C., Vandaele, A. C., Carleer, M., Fally, S., Colin, R., Jenouvrier, A., Coquart, B., and Mérienne, M.-F.: Absorption cross-sections of atmospheric constituents: NO_2, O_2, and H_2O, Environmental Science and Pollution Research, 6, 151–158, https://doi.org/10.1007/BF02987620, https://doi.org/10.1007/BF02987620, 1999.

Huan, L. and Kebin, H.: Traffic Optimization: A New Way for Air Pollution Control in China's Urban Areas, Environmental Science & Technology, 46, 5660–5661, https://doi.org/10.1021/es301778b, https://doi.org/10.1021/es301778b, pMID: 22612715, 2012.

Huang, R.-J., Zhang, Y., Bozzetti, C., Ho, K.-F., Cao, J.-J., Han, Y., Daellenbach, K. R., Slowik, J. G., Platt, S. M., Canonaco, F., et al.: High secondary aerosol contribution to particulate pollution during haze events in China, Nature, 514, 218–222, 2014.

Inness, A., Blechschmidt, A.-M., Bouarar, I., Chabrillat, S., Crepulja, M., Engelen, R. J., Eskes, H., Flemming, J., Gaudel, A., Hendrick, F., Huijnen, V., Jones, L., Kapsomenakis, J., Katragkou, E., Keppens, A., Langerock, B., de Mazière, M., Melas, D., Parrington, M., Peuch, V. H., Razinger, M., Richter, A., Schultz, M. G., Suttie, M., Thouret, V., Vrekoussis, M., Wagner, A., and Zerefos, C.: Data assimilation of satellite-retrieved ozone, carbon monoxide and nitrogen dioxide with ECMWF's Composition-IFS, Atmospheric Chemistry and Physics, 15, 5275–5303, https://doi.org/10.5194/acp-15-5275-2015, https://www.atmos-chem-phys.net/15/5275/2015/, 2015.

Jang, M. and Kamens, R. M.: Characterization of Secondary Aerosol from the Photooxidation of Toluene in the Presence of NO_x and 1-Propene, Environmental Science & Technology, 35, 3626–3639, https://doi.org/10.1021/es010676+, 2001.

Kaur, S., Nieuwenhuijsen, M., and Colvile, R.: Fine particulate matter and carbon monoxide exposure concentrations in urban street transport microenvironments, Atmospheric Environment, 41, 4781–4810, https://doi.org/10.1016/j.atmosenv.2007.02.002, http://www.sciencedirect.com/science/article/pii/S1352231007001343, 2007.

Kebabian, P. L., Herndon, S. C., and Freedman, A.: Detection of Nitrogen Dioxide by Cavity Attenuated Phase Shift Spectroscopy, Analytical Chemistry, 77, 724–728, https://doi.org/10.1021/ac048715y, https://doi.org/10.1021/ac048715y, pMID: 15649079, 2005a.

Kebabian, P. L., Herndon, S. C., and Freedman, A.: Detection of nitrogen dioxide by cavity attenuated phase shift spectroscopy, Analytical chemistry, 77, 724–728, 2005b.

Kebabian, P. L., Wood, E. C., Herndon, S. C., and Freedman, A.: A practical alternative to chemiluminescence-based detection of nitrogen dioxide: Cavity attenuated phase shift spectroscopy, Environmental science & technology, 42, 6040–6045, 2008.

Kirchstetter, T. W., Harley, R. A., Kreisberg, N. M., Stolzenburg, M. R., and Hering, S. V.: On-road measurement of fine particle and nitrogen oxide emissions from light-and heavy-duty motor vehicles, Atmospheric Environment, 33, 2955–2968, 1999.

https://doi.org/10.5194/acp-2019-1198
Preprint. Discussion started: 9 March 2020

Kraus, S.: DOASIS A Framework Design for DOAS, Ph.D. thesis, Combined Faculties for Mathematics and for Computer Science, University of Mannheim, 2005.

Krotkov, N. A., Lamsal, L. N., Celarier, E. A., Swartz, W. H., Marchenko, S. V., Bucsela, E. J., Chan, K. L., Wenig, M., and Zara, M.: The version 3 OMI NO_2 standard product, Atmospheric Measurement Techniques, 10, 3133–3149, https://doi.org/10.5194/amt-10-3133-2017, 2017.

Kuhlmann, G., Hartl, A., Cheung, H., Lam, Y., and Wenig, M.: A novel gridding algorithm to create regional trace gas maps from satellite observations, Atmospheric Measurement Techniques, 7, 451–467, 2014.

Kuhlmann, G., Lam, Y., Cheung, H., Hartl, A., Fung, J., Chan, P., and Wenig, M.: Development of a custom OMI NO 2 data product for evaluating biases in a regional chemistry transport model, Atmospheric Chemistry and Physics, 15, 5627–5644, 2015.

Kundu, S., Deming, B. L., Lew, M. M., Bottorff, B. P., Rickly, P., Stevens, P. S., Dusanter, S., Sklaveniti, S., Leonardis, T., Locoge, N., and Wood, E. C.: Peroxy Radical Measurements by Ethane – Nitric Oxide Chemical Amplification and Laser-Induced Fluorescence/Fluorescence Assay by Gas Expansion during the IRRONIC field campaign in a Forest in Indiana, Atmospheric Chemistry and Physics Discussions, 2019, 1–31, https://doi.org/10.5194/acp-2018-1359, https://www.atmos-chem-phys-discuss.net/acp-2018-1359/, 2019.

Lamsal, L., Martin, R., Van Donkelaar, A., Steinbacher, M., Celarier, E., Bucsela, E., Dunlea, E., and Pinto, J.: Ground-level nitrogen dioxide concentrations inferred from the satellite-borne Ozone Monitoring Instrument, Journal of Geophysical Research: Atmospheres, 113, 2008.

Langridge, J. M., Ball, S. M., and Jones, R. L.: A compact broadband cavity enhanced absorption spectrometer for detection of atmospheric NO_2 using light emitting diodes, Analyst, 131, 916–922, 2006.

Laughner, J. L. and Cohen, R. C.: Quantification of the effect of modeled lightning NO_2 on UV–visible air mass factors, Atmospheric Measurement Techniques, 10, 4403–4419, https://doi.org/10.5194/amt-10-4403-2017, https://www.atmos-meas-tech.net/10/4403/2017/, 2017.

LfU: Untersuchung der räumlichen Verteilung der NOx-Belastung im Umfeld von vorhandenen, hochbelasteten Luftmessstationen, Abschlussbericht, Tech. rep., Bayerisches Landesamt für Umwelt, 2015.

LfU, B.: Aktuelle Werte der bayerischen Luftmessstationen, https://www.lfu.bayern.de/luft/immissionsmessungen/messwerte/index.htm, accessed: 2019-11-29, 2019.

Lin, J.-T., Liu, Z., Zhang, Q., Liu, H., Mao, J., and Zhuang, G.: Modeling uncertainties for tropospheric nitrogen dioxide columns affecting satellite-based inverse modeling of nitrogen oxides emissions, Atmospheric Chemistry and Physics, 12, 12 255–12 275, https://doi.org/10.5194/acp-12-12255-2012, https://www.atmos-chem-phys.net/12/12255/2012/, 2012.

Marchenko, S., Krotkov, N. A., Lamsal, L. N., Celarier, E. A., Swartz, W. H., and Bucsela, E. J.: Revising the slant column density retrieval of nitrogen dioxide observed by the Ozone Monitoring Instrument, Journal of Geophysical Research: Atmospheres, 120, 5670–5692, https://doi.org/10.1002/2014JD022913, http://dx.doi.org/10.1002/2014JD022913, 2014JD022913, 2015.

Min, K.-E., Washenfelder, R. A., Dubé, W. P., Langford, A. O., Edwards, P. M., Zarzana, K. J., Stutz, J., Lu, K., Rohrer, F., Zhang, Y., and Brown, S. S.: A broadband cavity enhanced absorption spectrometer for aircraft measurements of glyoxal, methylglyoxal, nitrous acid, nitrogen dioxide, and water vapor, Atmospheric Measurement Techniques, 9, 423–440, https://doi.org/10.5194/amt-9-423-2016, https://www.atmos-meas-tech.net/9/423/2016/, 2016.

Ning, Z., Wubulihairen, M., and Yang, F.: PM, NO_x and butane emissions from on-road vehicle fleets in Hong Kong and their implications on emission control policy, Atmospheric Environment, 61, 265–274, https://doi.org/10.1016/j.atmosenv.2012.07.047, http://www.sciencedirect.com/science/article/pii/S1352231012007194, 2012.

https://doi.org/10.5194/acp-2019-1198
Preprint. Discussion started: 9 March 2020

Atmospheric Chemistry and Physics Discussions

Petritoli, A., Bonasoni, P., Giovanelli, G., Ravegnani, F., Kostadinov, I., Bortoli, D., Weiss, A., Schaub, D., Richter, A., and Fortezza, F.: First comparison between ground-based and satellite-borne measurements of tropospheric nitrogen dioxide in the Po basin, Journal of Geophysical Research: Atmospheres, 109, 2004.

Platt, U., Meinen, J., Pöhler, D., and Leisner, T.: Broadband Cavity Enhanced Differential Optical Absorption Spectroscopy (CE-DOAS) – applicability and corrections, Atmospheric Measurement Techniques, 2, 713–723, https://doi.org/10.5194/amt-2-713-2009, https://www.atmos-meas-tech.net/2/713/2009/, 2009.

Rakowska, A., Wong, K. C., Townsend, T., Chan, K. L., Westerdahl, D., Ng, S., Močnik, G., Drinovec, L., and Ning, Z.: Impact of traffic volume and composition on the air quality and pedestrian exposure in urban street canyon, Atmospheric Environment, 98, 260–270, https://doi.org/10.1016/j.atmosenv.2014.08.073, http://www.sciencedirect.com/science/article/pii/S1352231014006840, 2014.

Rothman, L., Barbe, A., Benner, D. C., Brown, L., Camy-Peyret, C., Carleer, M., Chance, K., Clerbaux, C., Dana, V., Devi, V., Fayt, A., Flaud, J.-M., Gamache, R., Goldman, A., Jacquemart, D., Jucks, K., Lafferty, W., Mandin, J.-Y., Massie, S., Nemtchinov, V., Newnham, D., Perrin, A., Rinsland, C., Schroeder, J., Smith, K., Smith, M., Tang, K., Toth, R., Auwera, J. V., Varanasi, P., and Yoshino, K.: The HITRAN molecular spectroscopic database: edition of 2000 including updates through 2001, Journal of Quantitative Spectroscopy and Radiative Transfer, 82, 5–44, https://doi.org/10.1016/S0022-4073(03)00146-8, http://www.sciencedirect.com/science/article/pii/S0022407303001468, the HITRAN Molecular Spectroscopic Database: Edition of 2000 Including Updates of 2001., 2003.

Silvern, R. F., Jacob, D. J., Mickley, L. J., Sulprizio, M. P., Travis, K. R., Marais, E. A., Cohen, R. C., Laughner, J. L., Choi, S., Joiner, J., and Lamsal, L. N.: Using satellite observations of tropospheric NO_2 columns to infer long-term trends in US NO_x emissions: the importance of accounting for the free tropospheric NO_2 background, Atmospheric Chemistry and Physics, 19, 8863–8878, https://doi.org/10.5194/acp-19-8863-2019, https://www.atmos-chem-phys.net/19/8863/2019/, 2019.

Thalman, R. and Volkamer, R.: Inherent calibration of a blue LED-CE-DOAS instrument to measure iodine oxide, glyoxal, methyl glyoxal, nitrogen dioxide, water vapour and aerosol extinction in open cavity mode, Atmospheric Measurement Techniques, 3, 1797–1814, https://doi.org/10.5194/amt-3-1797-2010, https://www.atmos-meas-tech.net/3/1797/2010/, 2010.

UBA: Air quality 2016 (Preliminary Evaluation), Tech. rep., Umweltbundesamt (German Environment Agency), jan.2017, 2017.

Uhrner, U., von Löwis, S., Vehkamäki, H., Wehner, B., Bräsel, S., Hermann, M., Stratmann, F., Kulmala, M., and Wiedensohler, A.: Dilution and aerosol dynamics within a diesel car exhaust plume-CFD simulations of on-road measurement conditions, Atmospheric Environment, 41, 7440–7461, https://doi.org/10.1016/j.atmosenv.2007.05.057, http://www.sciencedirect.com/science/article/pii/S1352231007005006, 2007.

Vandaele, A. C., Hermans, C., Fally, S., Carleer, M., Colin, R., Mérienne, M.-F., Jenouvrier, A., and Coquart, B.: High-resolution Fourier transform measurement of the NO_2 visible and near-infrared absorption cross sections: Temperature and pressure effects, Journal of Geophysical Research: Atmospheres, 107, ACH 3–1–ACH 3–12, https://doi.org/10.1029/2001JD000971, http://dx.doi.org/10.1029/2001JD000971, 4348, 2002.

Venables, D. S., Gherman, T., Orphal, J., Wenger, J. C., and Ruth, A. A.: High sensitivity in situ monitoring of NO_3 in an atmospheric simulation chamber using incoherent broadband cavity-enhanced absorption spectroscopy, Environmental science & technology, 40, 6758–6763, 2006.

Villena, G., Bejan, I., Kurtenbach, R., Wiesen, P., and Kleffmann, J.: Interferences of commercial NO_2 instruments in the urban atmosphere and in a smog chamber, Atmospheric Measurement Techniques, 5, 149–159, https://doi.org/10.5194/amt-5-149-2012, 2012.

https://doi.org/10.5194/acp-2019-1198
Preprint. Discussion started: 9 March 2020

Vogt, R., Scheer, V., Casati, R., and Benter, T.: On-Road Measurement of Particle Emission in the Exhaust Plume of a Diesel Passenger Car, Environmental Science & Technology, 37, 4070–4076, https://doi.org/10.1021/es0300315, https://doi.org/10.1021/es0300315, pMID: 14524437, 2003.

Volkamer, R., Spietz, P., Burrows, J., and Platt, U.: High-resolution absorption cross-section of glyoxal in the UV–VIS and IR spectral ranges, Journal of Photochemistry and Photobiology A: Chemistry, 172, 35–46, https://doi.org/10.1016/j.jphotochem.2004.11.011, http://www.sciencedirect.com/science/article/pii/S1010603004005143, 2005.

Washenfelder, R. A., Langford, A. O., Fuchs, H., and Brown, S. S.: Measurement of glyoxal using an incoherent broadband cavity enhanced absorption spectrometer, Atmospheric Chemistry and Physics, 8, 7779–7793, https://doi.org/10.5194/acp-8-7779-2008, https://www.atmos-chem-phys.net/8/7779/2008/, 2008.

Wenig, M. O., Cede, A., Bucsela, E., Celarier, E., Boersma, K., Veefkind, J., Brinksma, E., Gleason, J., and Herman, J.: Validation of OMI tropospheric NO2 column densities using direct-Sun mode Brewer measurements at NASA Goddard Space Flight Center, Journal of Geophysical Research: Atmospheres, 113, 2008.

Wesely, M. and Hicks, B.: A review of the current status of knowledge on dry deposition, Atmospheric environment, 34, 2261–2282, 2000.

Westerdahl, D., Fruin, S., Sax, T., Fine, P. M., and Sioutas, C.: Mobile platform measurements of ultrafine particles and associated pollutant concentrations on freeways and residential streets in Los Angeles, Atmospheric Environment, 39, 3597–3610, https://doi.org/10.1016/j.atmosenv.2005.02.034, http://www.sciencedirect.com/science/article/pii/S1352231005002232, 2005.

Xie, C., Xu, W., Wang, J., Wang, Q., Liu, D., Tang, G., Chen, P., Du, W., Zhao, J., Zhang, Y., Zhou, W., Han, T., Bian, Q., Li, J., Fu, P., Wang, Z., Ge, X., Allan, J., Coe, H., and Sun, Y.: Vertical characterization of aerosol optical properties and brown carbon in winter in urban Beijing, China, Atmospheric Chemistry and Physics, 19, 165–179, https://doi.org/10.5194/acp-19-165-2019, https://www.atmos-chem-phys.net/19/165/2019/, 2019.

Zara, M., Boersma, K. F., De Smedt, I., Richter, A., Peters, E., van Geffen, J. H. G. M., Beirle, S., Wagner, T., Van Roozendael, M., Marchenko, S., Lamsal, L. N., and Eskes, H. J.: Improved slant column density retrieval of nitrogen dioxide and formaldehyde for OMI and GOME-2A from QA4ECV: intercomparison, uncertainty characterisation, and trends, Atmospheric Measurement Techniques, 11, 4033–4058, https://doi.org/10.5194/amt-11-4033-2018, https://www.atmos-meas-tech.net/11/4033/2018/, 2018.

Zhu, Y., Chan, K. L., Lam, Y. F., Horbanski, M., Pöhler, D., Boll, J., Lipkowitsch, I., Ye, S., and Wenig, M.: Analysis of spatial and temporal patterns of on-road NO_2 concentrations in Hong Kong, Atmospheric Measurement Techniques, 11, 6719–6734, https://doi.org/10.5194/amt-11-6719-2018, https://www.atmos-meas-tech.net/11/6719/2018/, 2018.